Decomposed Velocity Field in $f(R)$ Gravity

XiaoQi Yu[1]

[1]*Gustavus Adolphus College, 800 West College Avenue, St.Peter, MN 56082, USA*

Abstract

We propose a new method to distinguish modified gravity $f(R)$ cosmology from ΛCDM cosmology. N-body simulations are performed to predict the density and velocity field of these cosmologies. By decomposing peculiar velocity in the simulations into three eigen-components, an irrotational component completely correlated with the density field V_δ, an irrotational component completely uncorrelated with density field V_S, and a rotational component V_B, the velocity power spectra of these components are compared and contrasted for different cosmology models. A close investigation of the contrast among cosmological models for three components at shows that the V_S component is the most powerful one to indicate $f(R)$ cosmology. We find that, even for an $f(R)$ model with $|f_{R0}| = 10^{-6}$, the power spectrum of V_S component can reach 13% higher than General Relavity at k=0.2h/Mpc. The differences between f(R) and GR in the V_S get larger as the scales get smaller. This signal is significant and could be checked in forthcoming observational data, which promises a new way to constrain the gravity models.

PACS numbers: Valid PACS appear here

I. INTRODUCTION

The origin of the observed late-time accelerated expansion of the universe has been an interesting question in theoretical physics [1–3]. The ΛCDM model, which is based on General Relativity (hereafter GR) and Standard Model of particle physics by including a cosmological constant term Λ, can well explain this phenomenon[4]. Although GR has been tested to high accuracy on solar scale, the assumption in the ΛCDM diagram that GR is valid on galactic and cosmological scales, however, has not been verified yet. Moreover, given that the assumption is true, the vacuum energy density predicted by particle physics theory on quantum scale is orders of magnitude larger than the cosmological inferred value for the cosmological constant. To resolve this, theories involve modifications on GR at galactic and cosmological scales are raised in recent years [5–8].

A well-studied attempt to modify GR is described by the $f(R)$ model, in which the Ricci scalar R in the standard Einstein-Hilbert action is replaced by a function $f(R)$. Since GR has been confirmed to high accuracy locally, deviations from GR caused by any modification must be minimum at small scale [9]. In $f(R)$, the modification to GR can be considered as if there exist a fictitious fifth force exerting at very short (sub-millimeter) range with very weak strength, and a screening mechanism, called chameleon, is employed to suppress the fifth force in regions with high matter density in order to match with GR [10–12]. The background expansion history in modified gravity theory should be also indistinguishable from that of ΛCDM to explain the accelerated expansion. However, the cosmological behaviors, such as structure formation history, can be different for the two scenarios[13]. It is hence crucial to investigate various cosmological behaviors to differentiate the two cosmologies.

Previous attempts on this subject include measuring the matter and velocity power spectrum, the redshift distortion, the weak lensing, the pair-wise galaxy velocity, and the Minkowski Functionals in different cosmologies [14–20]. In this work, we investigate the statistics of the cosmic peculiar velocity in both $f(R)$ and GR cosmologies. The cosmic peculiar velocity field conveys cosmological information; it indicates the growth rate and the structure formation history of the universe, which makes a good candidate to separate different gravity and dark energy models [21–26]. In this work, we decompose the cosmic velocity field into three eigencomponents, a component that is completely correlated with the underlying cosmic density field V_δ, an irrotational component completely uncorrelated with density field V_S, and a rotational component V_B [27, 28]. Such decomposition has been previously employed to reconstruct redshift space distor-

tion, and the three components have been show to have different origin and scale dependence. The imprints of cosmic perturbation on structure formation at various scales can therefore be better presented with the decomposition. Using the fact that the chameleon mechanism in $f(R)$ is employed at high density region, we can expected that the cosmic velocity fields in $f(R)$ to deviate from that in GR on some certain scale presented in the decomposition.

In this study, we sample the statistics of decomposed velocity field in a set of $f(R)$ and GR cosmological simulations using the ECOSMOG code[29]. In order to distinguish different gravity models, we measure the deviation of the power spectra of velocity components in $f(R)$ from those in GR cosmologies.

This work is outlined as following: in Section II we give a short summary of the $f(R)$ theory. Section III presents the velocity field decomposition method and its physical implication in cosmology. The simulations used for the study is summarized in Section IV. Section V discusses the treatment of the simulation result in order to obtain the statistics of the decomposed velocity field, and we compared and contrasted the statistics between FR and $f(R)$ in Section VI. We summarize and discuss in Section VII.

II. THE $f(R)$ GRAVITY MODEL

III. THE VELOCITY DECOMPOSITION

Any vector field can be decomposed into a divergence (irrotational) component and a curl (rotational) component. Analogous to the electric and magnetic fields, we denote the divergence component with a subscript **E** and the curl component with a subscript **B** [26, 27]. Hence, the peculiar velocity field can be decomposed into first order

$$\mathbf{v}(\mathbf{x}) = \mathbf{v_E}(\mathbf{x}) + \mathbf{v_B}(\mathbf{x}), \tag{1}$$

in which the E-mode component is curl free $\nabla \times \mathbf{v_E} = 0$, and the B-mode component is divergence free ($\nabla \cdot \mathbf{v_B} = 0$). In fourier space, we have

$$\mathbf{v_E}(\mathbf{k}) = \frac{\mathbf{k} \cdot \mathbf{v}(\mathbf{k})}{k^2}\mathbf{k} \tag{2}$$

$$\mathbf{v_B}(\mathbf{k}) = \mathbf{v}(\mathbf{k}) - \mathbf{v_E}(\mathbf{k}). \tag{3}$$

The divergence component $\mathbf{v_E}$ can be completely described by the velocity divergence

$\theta(\mathbf{x}) \equiv \nabla \cdot \mathbf{v}(\mathbf{x})/H \equiv \nabla \cdot \mathbf{v_E}(\mathbf{x})/H$. We can hence further decompose $\mathbf{v_E}$ into two second order components to demonstrate the velocity-density relationship in cosmic field:

$$\mathbf{v_E}(\mathbf{x}) = \mathbf{v}_\delta(\mathbf{x}) + \mathbf{v_S}(\mathbf{x}), \tag{4}$$

where both components are also irrotational as $\mathbf{v_E}$. The divergence of $\mathbf{v}_\delta$, $\theta_\delta \equiv -\nabla \cdot \mathbf{v}_\delta/H$, is completely correlated with the underlying density field δ, whereas $\mathbf{v_S}$ is completely uncorrelated with the density field. We have therefore, the divergence of $\mathbf{v}_\delta$ in fourier space that

$$\theta_\delta(\mathbf{k}) = \delta(\mathbf{k})W(\mathbf{k}), \tag{5}$$

where $W(\mathbf{k})$ is a function of $\mathbf{k}$ determined by the cross-correlation between the density and velocity field. In order to calculated $W(\mathbf{k})$, we define the power spectrum between two fields A and B as $\langle A(\mathbf{k})B(\mathbf{k}')\rangle \equiv (2\pi)^3\delta_{3D}(\mathbf{k}+\mathbf{k}')P_{AB}(\mathbf{k})$. We usually present in the variance form $\Delta^2_{AB} \equiv k^3 P_{AB}/(2\pi^2)$ to make it convenient to calculate the assemble average as $\langle A(\mathbf{x})B(\mathbf{x})\rangle = \int \Delta^2_{AB}(k)dk/k$. Through the relationship $\langle\delta(\mathbf{k}')\theta(\mathbf{k})\rangle = \langle\delta(\mathbf{k}')\theta_\delta(\mathbf{k})\rangle = \langle\delta(\mathbf{k}')\delta(\mathbf{k})\rangle W(\mathbf{k})$, we obtain

$$W(\mathbf{k}) = W(k) = \frac{P_{\delta\theta}(k)}{P_{\delta\delta}(k)} \tag{6}$$

Notice that the universe is isotropic, hence $P_{\delta\theta}(\mathbf{k}) = P_{\delta\theta}(k)$ and $P_{\delta\delta}(\mathbf{k}) = P_{\delta\delta}(k)$. W has no angular dependence.

To summarize, in fourier space, we have for $\mathbf{v}_\delta$ and $\mathbf{v_S}$

$$\mathbf{v}_\delta(\mathbf{k}) = i\frac{\delta(\mathbf{k})W(k)H}{k^2}\mathbf{k} \tag{7}$$

$$\mathbf{v_S}(\mathbf{k}) = \mathbf{v_E}(\mathbf{k}) - \mathbf{v}_\delta(\mathbf{k}). \tag{8}$$

The $\mathbf{v}_\delta$ component is therefore completely correlated with the underlying density field, whereas the $\mathbf{v_S}$ component is completely uncorrelated with the density field, $\langle\theta_\mathbf{S}(\mathbf{x})\delta(\mathbf{x}+\mathbf{r})\rangle = 0$, make it the source of stochasticity in the velocity-density relationship.

In the limit of $k \ll k_{NL}$, where k_{NL} represent nonlinear scale defined by $\Delta^2_{\delta\delta}(k_{NL}) = 1$, which is about $k = 0.2$ for present redshift, $\mathbf{v}_\delta$ is expected to be the only velocity component. $\mathbf{v_B}$ is the curl component, hence it is expected to grow only after shell crossing. On the other hand, according to the linear perturbation theory, $\nabla \cdot \mathbf{v_E}/H \equiv \theta = f\delta$ in the linear regime, hence $\mathbf{v_E}$ should be completely correlated with the density field at $k \ll k_{NL}$. Therefore, $\mathbf{v_S}$ is also expected to vanish. $\mathbf{v}_\delta$ then is of the greatest interest for the large scale structure growth. By comparing

$\mathbf{v}_\delta$ in $f(R)$ and GR model at large scale, we can probe the linear structure formation of these two cosmology.

To the opposite of $\mathbf{v}_\delta$, the $\mathbf{v_S}$ vanishes in the linear regime and begins to grow due to the nonlinear evolution. It is expected to emerge at the quasilinear scale $k \approx k_{NL}$, makes it crucial to test modified gravity. For modified gravity models to pass the local tests and to drive the late time cosmic acceleration, gravity must behave upon the environment. The environmental dependence emerges to be important at the quasilinear scales. Arisen from nonlinear evolution, $\mathbf{v_S}$ can tell us the formation history at the galactic scale, making it a good candidate for testing gravity.

The $\mathbf{v_B}$ component grows only when the nonlinearity is sufficiently large that the shell crossing happens. We expect that its power concentrate at smaller scales than $\mathbf{v_S}$. Since $\mathbf{v_B}$ is caused by virialization and shell crossing at the scale smaller than local test, it is expected that $\mathbf{v_B}$ is of less significance in probing modified gravity.

Figure 1 shows the power spectra of velocity components from the two step decomposition of the peculiar velocity field in Equation 1 and 4. The power spectra is measured in a simulation output with GR cosmology, represented in Fourier space. The power spectra of the velocity component agree with the predictions from perturbation theory by showing that $\mathbf{v}_\delta$ dominates at linear scale, $\mathbf{v_S}$ begins to grow from nonlinear effect, and $\mathbf{v_B}$ only grows when nonlinearity is sufficiently large. We have thus show that the velocity decomposition into three components are mathematically unique, and physically meaningful to indicating the structure formation history in different cosmologies.

IV. NUMERICAL SIMULATION

This study uses the ELEPHANT simulation. Each set of simulation includes three simulations with distinct models, one using ΛCDM model, and two using $f(R)$ gravity with $|f_{R0}| = 10^{-6}$ and 10^{-5}, which will be referred as GR, F6 and F5 respectively. In the perturbation theory, we expect that $\mathbf{v}_\delta$ to dominate at linear scales and $\mathbf{v_S}$ and $\mathbf{v_B}$ to emerge and later dominate at nonlinear scales. Thus, it would be difficult to robustly quantify all three components in one set of simulations with only one box size. A good remedy is to combine large box simulations with small box simulations, where the large box simulations will help us to quantify the deviations of $f(R)$ from GR at large scales, especially for the $\mathbf{v}_\delta$ component, and the small box simulations will have higher mass and force resolution, helping us to probe deviation at small scales for $\mathbf{v_B}$ components.

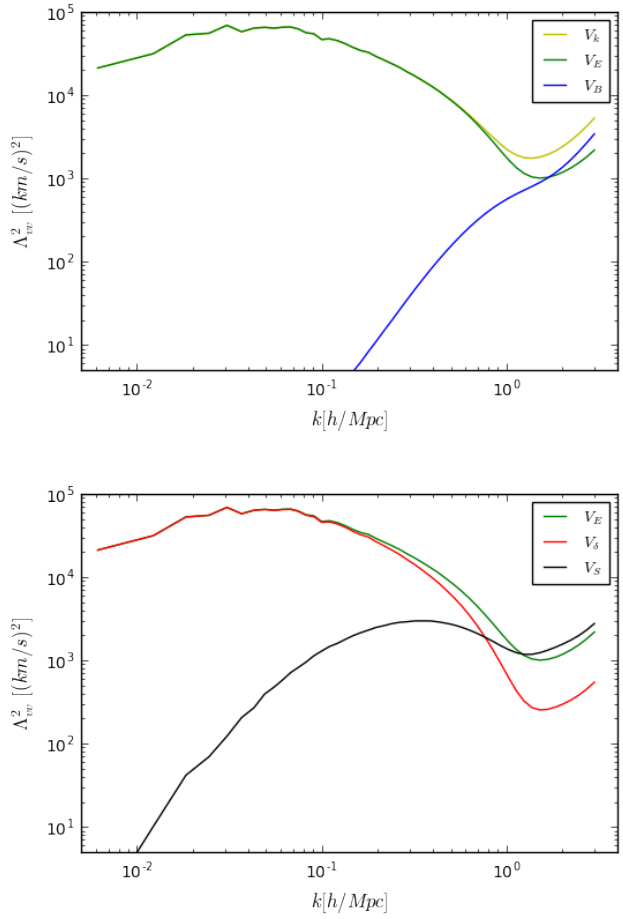

Figure 1: Upper panel: The power spectra of sampled velocity field $\mathbf{v_k}$ and its first order decomposition into $\mathbf{v_E}$ and $\mathbf{v_B}$. Lower panel: the power spectra of divergence velocity component $\mathbf{v_E}$ and the second order decomposition of the $\mathbf{v_E}$ into $\mathbf{v}_\delta$ and $\mathbf{v_S}$. The velocity field is sampled from a simulation output with ΛCDM cosmology at current redshift.

For the above reason, in each set of the simulations, $N_p = 1024^3$ particles are evolved in a cubic box, starting from exactly the same initial conditions at z = 49.0. The box sizes for these simulations are $L_{box}/h^{-1}Mpc$ =1024, 900, 450, and 250 per side, which will be refered as B1024, B900, B450, and B250 respectively in future discussion. The simulations are performed with the adaptive mesh refinement code ECOSMOG.which is covered by a regular mesh with 1024^3 cells. The cells are refined if they contain more than 8 particles, and such an adaptive refinement scheme ensures high force resolution in dense regions, where modified gravity effects are hard to calculate. The cosmological parameters set for the simulations in B1024, B900, and B450 are: Ω_m = 0.281, Ω_Λ= 0.719, h = 0.697, n_S =0.971 and σ_8 = 0.820. The paramters set for B250 are: Ω_m = 0.267,

Ω_Λ= 0.733, h = 0.71, n_S =0.958 and σ_8 = 0.801. The first two are the dimensionless energy density of non-relativistic matter and dark energy, h is the dimensionless hubble parameter, n_S is the spectral index of the primordial power spectrum and σ_8 is the rms density fluctuation measured in a sphere of radius r=8 Mpc/h at z=0.

V. THE POWER SPECTRA OF DECOMPOSED VELOCITY FIELD

A. The Density and Velocity Assignment

It is tricky to sample velocity field statistics from discrete and clustered distribution of halos and galaxies. Limited particles in N-body simulation leave voids in the particle field where there's no velocity information. However, the velocity at void is not necessary negligible. In contrast, since the unvirialized velocity is correlated with the underlying large-scale matter distribution, velocity at void can be large. In order to avoid zero velocity, we use the nearest-particle (NP) method to sample velocity statistics:after constructing uniform grid in the simulation box, we assign the velocity of the nearest dark matter particle to the grid points. Notice that the NP-method constructs a volume-weighted velocity field by that the probability P of a particle assigned to a grid is proportional to the volume V the particle occupied. The density field δ is sample by nearest-grid-point (NGP) method on the same grids as the velocity field sampling.

B. Testing the Sampling Method

We carried out several tests to verify the robustness of the NP method and determine the reliable ranges of k for each velocity components in our study. For the divergence velocity component, large box simulations are needed to sufficiently sample the velocity field. Going into small scales for $\mathbf{v_B}$, high mass resolution is needed to capture the shell-crossing. Previous study by Zheng [28] shows that the NP method can reliably construct $\mathbf{v}_\delta$ and $\mathbf{v_S}$ components in large box simulation, and $\mathbf{v_B}$ can be reasonably constructed in box size of 100Mpc/h. Here, in order to sample the velocity field on a wide range of scales, we test convergence for all components from large scale (small k) in big box down to small scale (large k) in small box with the GR simulations. For large scale, convergence test against grid number $N_{grid} = 256^3, 512^3, 1024^3$ in B1024 is performed to check if the power spectra of velocity is sensitive to sampling artifacts. We do the same thing for small scale(large k) with B250. To check if large box and small box simulations are consistent,

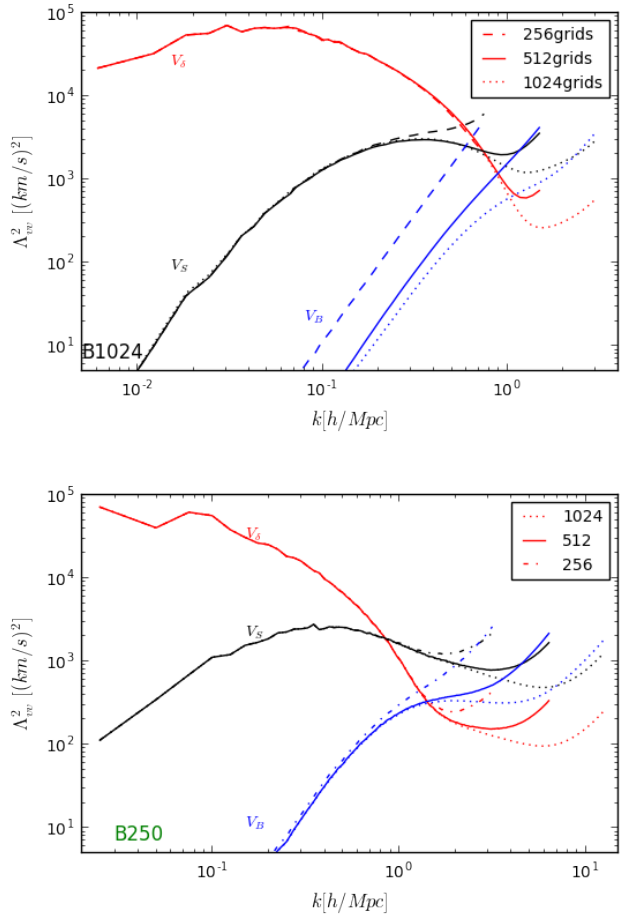

Figure 2: The power spectra of velocity components with GR simulation. Top:The figure is intend for test convergence on the grid size in 1024 Mpc/h box. Bottom: Convergence tests on the grid size in 250 Mpc/h box. The plot is binned along k- axis linearly for small k and logistically for large k. The data points are at the linear center of each bin. Fine grids are required to robustly sample the velocity and density field. For a given grid size, we should only trust the regimes where the result agress with that of finer grids. Tests against grid sizes show that 512^3 grid of B1024 are needed to measure $\mathbf{v}_\delta$ and $\mathbf{v_S}$ at $k \leq 0.8$ h/Mpc. Going into small scale with B250, 512^3 grids are needed to measure $\mathbf{v_B}$ at $k \leq 1$ h/Mpc

we test convergence with same grid number against various box sizes in Figure 3 for box size of B1024, B900, and B450.

As shown in Figure 2(a) and 2(b), the gridsize associated artifacts in $\mathbf{v}_\delta$ and $\mathbf{v_S}$ are negligible for $k \leq 0.8$ h/Mpc with grid number $N_{grid} = 512^3$ in B1024. For the $\mathbf{v_B}$ component, no convergence is found in B1024; even in B250, there's no convergence until N_{grid} reaches 512^3 with $k \leq 1$ h/Mpc. In Figure 3, we plot the convergence test against box sizes with $N_{grid} = 512^3$; the $\mathbf{v}_\delta$

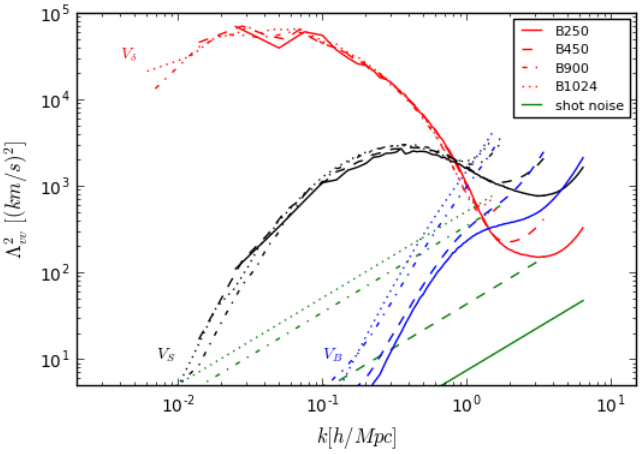

Figure 3: Consistency tests on the box size from 1024 Mpc/h to 450 Mpc/h with $N_{grid} = 512^3$, in which the simulations share the same cosmological parameters and initial condition for realization. The green lines shows the Poisson noise associated with the box size of the simulation. For convenience, the power spectra of velocity components measured in box of 250Mpc/h are also plotted here in order to show its validity to sample $\mathbf{v_B}$ component, although the B250 simulation uses different cosmological parameter. Comparison between box sizes shows that $\mathbf{v}_\delta$ and $\mathbf{v_S}$ components lose their power at $k \approx 1$ h/Mpc in B1024 due to the low resolution. B1024 with grid size of 512^3 can properly sample the velocity statistics of these two components in range of $k = [0.01 : 0.8]$ h/Mpc. The $\mathbf{v_B}$ components in all but B250 simulations have parts that are below the Poisson noise. For this reason, we use B250 to sample $\mathbf{v_B}$. B250 with 512^3 grids can give us proper measurement of $\mathbf{v_B}$ on scale of $k = [0.2 : 1]$ h/Mpc

and $\mathbf{v_S}$ components converge from B1024 down to B450 for $k = [0.01, 0.8]$ h/Mpc with minor discrepancies. The $\mathbf{v_B}$ components in all but B250 simulations have parts that are below the Poisson noise. For this reason, we use B250 to sample $\mathbf{v_B}$.

Hence, the NP method can reliably construct the velocity on wide range of scales by combining B1024 and B250 simulations. $\mathbf{v}_\delta$ and $\mathbf{v_S}$ components are sampled by B1024 with $N_{grid} = 512^3$ on scale of $k = [0.01, 0.8]$ h/Mpc, and the $\mathbf{v_B}$ is sampled at $k = [0.2, 1]$ h/Mpc using B250 with $N_{grid} = 512^3$.

VI. COMPARING GR AND $f(R)$

The shape of the matter and velocity power spectra are sensitive to changes in cosmological parameters [30]. In principle, the difference between power spectra for $f(R)$ and GR could

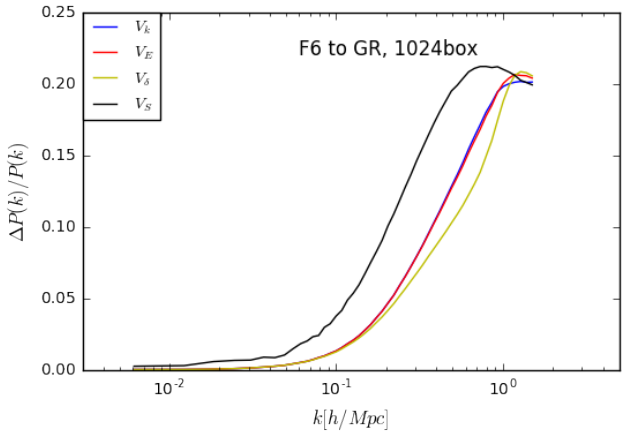

(a)F6 to GR

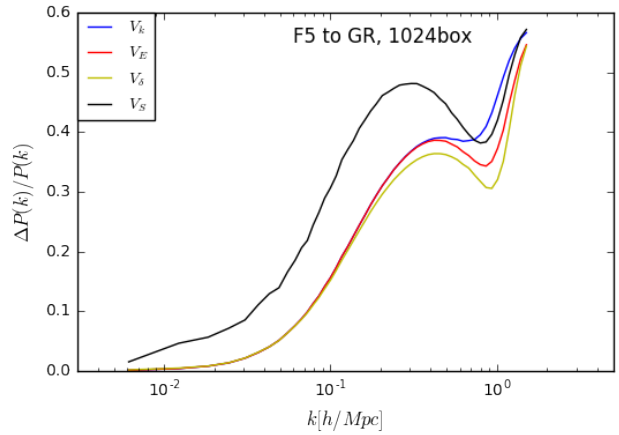

(b)F5 to GR

Figure 4: The relative difference between the power spectra of velocity fields (represented in Fourier space as $\mathbf{v_k}$) and its $\mathbf{v_E}$, $\mathbf{v}_\delta$ and $\mathbf{v_S}$ components measured $f(R)$ and those measured in GR with simulations of boxsize 1024 Mpc/h. The upper panel shows the relative difference between F6 and ΛCDM simulations and the lower panel shows the relative difference between F5 and ΛCDM simulations. In both F5 and F6, the contrast is the highest for $\mathbf{v_S}$ on scale of $k = [0.01 : 0.8]$ h/Mpc among all components.

be degenerated with the effect of changing cosmological parameters. However, with the current precision of observations, the effects of cosmological parameters on the power spectra can be distinguished by CMB data with eg. Planck [31, 32]. Hence, here we can focus on the difference between power spectra for $f(R)$ and GR by looking at the shape of contrast $\Delta P(k)/P(k)$, where $\Delta P(k)$ is the difference between the power spectra for $f(R)$ gravity and ΛCDM, defined as

$$\frac{\Delta P(k)}{P(k)} \equiv \frac{\Delta^2_{vv}(k)\mathbf{f(R)}}{\Delta^2_{vv}(k)\mathbf{\Lambda CDM}} - 1 \tag{9}$$

The results for the relative differences of the velocity field and its $\mathbf{v_E}$, $\mathbf{v}_\delta$ and $\mathbf{v_S}$ components between $f(R)$ and GR measured in B1024 are shown in Figure 4. The effect of modified gravity on $\mathbf{v_S}$ is the greatest on the scale of $k = [0.01 : 0.8]$ h/Mpc. At $k = 0.2$ h/Mpc where the imprint of nonlinear evolution begin to partake, the contrast for $\mathbf{v_S}$ already reaches 13.3% for F6 and 53.3% for F5. The contrast continues to grow to the largest and then drop. The environmental dependence nature of $f(R)$ is most obvious through the $\mathbf{v_S}$ component.

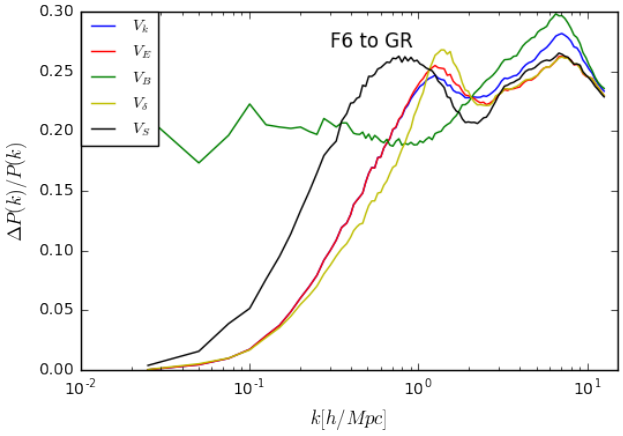

(a)F6 to GR

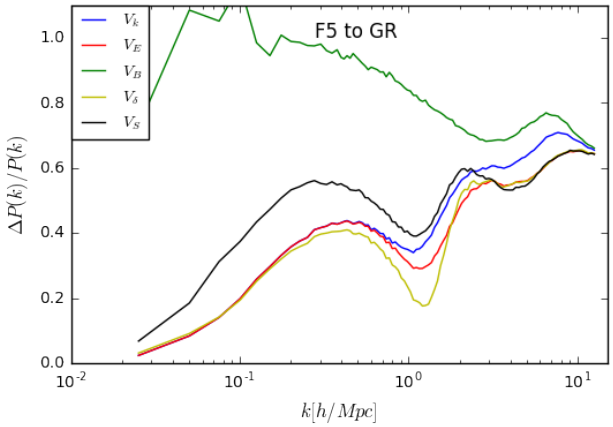

(b)F5 to GR

Figure 5: The relative difference between the power spectra of velocity fields (represented in Fourier space as $\mathbf{v_k}$) and its all components measured $f(R)$ and those measured in GR cosmology simulations of boxsize 250 Mpc/h. The upper panel shows the relative difference between F6 and ΛCDM simulations and the lower panel shows the relative difference between F5 and ΛCDM simulations. In F5, the contrast for $\mathbf{v_B}$ is the highest on scale of $k = [0.2 : 1]$ h/Mpc among all components, however, in F6, the contrast for $\mathbf{v_B}$ is the lowest among all components on scale of $k = [0.2 : 1]$ h/Mpc.

Figure 5 shows the relative differences of the velocity field and its all components between $f(R)$ and GR measured in box of 250 Mpc/h. The range of scale we can trust for the $\mathbf{v_B}$ component is $k = [0.2 : 1]$ h/Mpc in B250. While the $\mathbf{v_B}$ components has the highest relative difference among all components in F5, the relative difference in $\mathbf{v_B}$ is the smallest in F6 for the reliable range of scale. Therefore, we cannot rely on the $\mathbf{v_B}$ for the purpose of probing $f(R)$.

VII. CONCLUSION AND SUMMARY

In this study, we combine $f(R)$ (F5, F6) and GR simulations in boxes of 1024 Mpc/h and 250 Mpc/h to construct the decomposed velocity field of the large scale structure using Nearest Particle interpolation to the grids. By examing the deviation of the decomposed velocity power spectra of $f(R)$ from GR, we find that $\mathbf{v_S}$ is significant to probe gravity at galactic and cosmological scales among all components. At $k = 0.2$ h/Mpc where the imprint of nonlinear evolution begin to partake, the contrast for $\mathbf{v_S}$ already reaches 13.3% for F6 and 53.3% for F5. Our results hence suggest that the cosmic velocity field will be a powerful tool to study the nature of gravity when future redshift survey is available.

[1] A. G. Riess, A. V. Filippenko, P. Challis, A. Clocchiatti, A. Diercks, P. M. Garnavich, R. L. Gilliland, C. J. Hogan, S. Jha, R. P. Kirshner, et al., Astrophys. J. **116**, 1009 (1998), astro-ph/9805201.

[2] S. Perlmutter, G. Aldering, M. della Valle, S. Deustua, R. S. Ellis, S. Fabbro, A. Fruchter, G. Goldhaber, D. E. Groom, I. M. Hook, et al., Nature (London) **391**, 51 (1998), astro-ph/9712212.

[3] S. Perlmutter, G. Aldering, G. Goldhaber, R. A. Knop, P. Nugent, P. G. Castro, S. Deustua, S. Fabbro, A. Goobar, D. E. Groom, et al., Astrophys. J. **517**, 565 (1999), astro-ph/9812133.

[4] E. J. Copeland, M. Sami, and S. Tsujikawa, International Journal of Modern Physics D **15**, 1753 (2006), hep-th/0603057.

[5] T. Clifton, P. G. Ferreira, A. Padilla, and C. Skordis, Phys. Rept. **513**, 1 (2012), 1106.2476.

[6] S. M. Carroll, V. Duvvuri, M. Trodden, and M. S. Turner, Phys. Rev. D **70**, 043528 (2004), astro-ph/0306438.

[7] A. Joyce, L. Lombriser, and F. Schmidt, Annual Review of Nuclear and Particle Science **66**, 95 (2016), 1601.06133.

[8] A. Joyce, B. Jain, J. Khoury, and M. Trodden, Phys. Rept. **568**, 1 (2015), 1407.0059.

[9] C. M. Will, Living. Rev. Rel. **17**, 4 (2014), 1403.7377.

[10] B. Li and J. D. Barrow, Phys. Rev. D **75**, 084010 (2007), gr-qc/0701111.

[11] J. Khoury and A. Weltman, Phys. Rev. D **69**, 044026 (2004), astro-ph/0309411.

[12] W. Hu and I. Sawicki, Phys. Rev. D **76**, 064004 (2007), 0705.1158.

[13] B. Jain and P. Zhang, Phys. Rev. D **78**, 063503 (2008), 0709.2375.

[14] W. Fang, B. Li, and G.-B. Zhao, Phys. Rev. Lett. **118**, 181301 (2017), 1704.02325.

[15] B. Li, W. A. Hellwing, K. Koyama, G.-B. Zhao, E. Jennings, and C. M. Baugh, Mon. Not. R. Astron. Soc. **428**, 743 (2013), 1206.4317.

[16] H. Oyaizu, M. Lima, and W. Hu, Phys. Rev. D **78**, 123524 (2008), 0807.2462.

[17] F. Schmidt, M. Lima, H. Oyaizu, and W. Hu, Phys. Rev. D **79**, 083518 (2009), 0812.0545.

[18] C. Ling, Q. Wang, R. Li, B. Li, J. Wang, and L. Gao, Phys. Rev. D **92**, 064024 (2015), 1410.2734.

[19] E. Jennings, C. M. Baugh, B. Li, G.-B. Zhao, and K. Koyama, Mon. Not. R. Astron. Soc. **425**, 2128 (2012), 1205.2698.

[20] W. A. Hellwing, B. Li, C. S. Frenk, and S. Cole, Mon. Not. R. Astron. Soc. **435**, 2806 (2013), 1305.7486.

[21] R. Reyes, R. Mandelbaum, U. Seljak, T. Baldauf, J. E. Gunn, L. Lombriser, and R. E. Smith, Nature (London) **464**, 256 (2010), 1003.2185.

[22] Y. Wang, J. Cosmo. Astropart. Phys. **5**, 021 (2008), 0710.3885.

[23] P. Zhang, M. Liguori, R. Bean, and S. Dodelson, Phys. Rev. Lett. **99**, 141302 (2007), 0704.1932.

[24] L. Guzzo, M. Pierleoni, B. Meneux, E. Branchini, O. Le Fèvre, C. Marinoni, B. Garilli, J. Blaizot, G. De Lucia, A. Pollo, et al. (????).

[25] E. V. Linder and A. Jenkins, Mon. Not. R. Astron. Soc. **346**, 573 (2003), astro-ph/0305286.

[26] Y. Yu, J. Zhang, Y. Jing, and P. Zhang, Phys. Rev. D **92**, 083527 (2015), 1505.06827.

[27] P. Zhang, J. Pan, and Y. Zheng, Phys. Rev. D **87**, 063526 (2013), 1207.2722.

[28] Y. Zheng, P. Zhang, Y. Jing, W. Lin, and J. Pan, Phys. Rev. D **88**, 103510 (2013), 1308.0886.

[29] B. Li, G.-B. Zhao, R. Teyssier, and K. Koyama, J. Cosmo. Astropart. Phys. **1**, 051 (2012), 1110.1379.

[30] D. J. Eisenstein and W. Hu, Astrophys. J. **511**, 5 (1999), astro-ph/9710252.

[31] P. Collaboration, Astronomy & Astrophysics **594**, A13 (2016), 1502.01589.

[32] P. Collaboration, ArXiv e-prints (2018), 1807.06209.